APPENDIX A
Vensim equations for the MONTE model

The MONTE model is a system dynamics model, written in Vensim language. Its equations with units of measurement are listed below.

DEPTH CORRECTION FACTOR = 1 Units: Dmnl (36)
FINAL TIME = 120 Units: Minute (37)
GRAVITATIONAL ACCELERATION = 9.8 Units: m/(s*s)
(38)
INITIAL DISTANCE PROPAGATED = 0 Units: m (39)
INITIAL TIME = 0 Units: Minute (40)
INITIAL WAVE HEIGHT = 1.5 Units: m (41)
MAXIMUM WAVE HEIGHT = 6 Units: m (42)
SOURCE DEPTH = 527 Units: m (43)
TIME CONVERSION FACTOR = 60 Units: s/Minute (44)
TIME STEP = 0.03125 Units: Minute (45)
TOTAL DISTANCE = 544710 Units: m (46)
VELOCITY CORRECTION FACTOR = 1.6Units: Dmnl (47)

Distance Propagated = INTEG(wave celerity,
INITIAL DISTANCE PROPAGATED) Units: m (48)

local water depth = (effect of distance on depth *
SOURCE DEPTH) Units: m (49)

potential wave height = INITIAL WAVE HEIGHT * SQRT(SQRT
(SOURCE DEPTH/local water depth)) Units: m (50)

relative distance = Distance Propagated/
TOTAL DISTANCE Units: Dmnl (51)

wave celerity = IF THEN ELSE(local water depth > 50, SQRT
(GRAVITATIONAL ACCELERATION * (wave height +
(local water depth * DEPTH CORRECTION FACTOR))) *
TIME CONVERSION FACTOR, VELOCITY CORRECTION FACTOR *
SQRT(GRAVITATIONAL ACCELERATION * (wave height +
(local water depth * DEPTH CORRECTION FACTOR))) *
TIME CONVERSION FACTOR) Units: m/Minute (52)

wave height = MIN(potential wave height, MAXIMUM WAVE HEIGHT) Units: m (53)

effect of distance on depth = WITH LOOKUP(relative distance, ([(0,0)(1.2,5.04357)],(0,1),(0.00783193,1.0541),(0.0156634,0.636126),(0.0234943,0.804125),(0.0313247,1.81906),(0.0391546,3.88361),(0.046984,4.47011),(0.0548129,4.62955),(0.0626412,5.04357),(0.0704691,4.93504),(0.0782964,4.83528),(0.0861232,4.23365),(0.0939495,4.36503),(0.101775,3.84451),(0.109601,3.88547),(0.117425,3.55443),(0.125249,3.33724),(0.133073,3.04497),(0.140896,2.92535),(0.148719,2.72369),(0.156541,2.33085),(0.164362,2.45544),(0.172183,1.81986),(0.180004,0.345365),(0.187824,1.06789),(0.195643,0.967627),(0.203462,0.749606),(0.21128,0.803046),(0.219098,0.973205),(0.226915,2.47862),(0.234732,2.96307),(0.242548,2.52339),(0.250363,1.65518),(0.258178,0.307644),(0.265993,1.63057),(0.273806,1.95526),(0.28162,2.81282),(0.289432,3.17195),(0.297245,3.22311),(0.305056,3.19811),(0.312867,3.2703),(0.320678,3.11306),(0.328487,3.05779),(0.336297,2.79868),(0.344106,2.79721),(0.351914,2.63188),(0.359721,2.45669),(0.367528,2.41399),(0.375335,2.48735),(0.383141,2.38617),(0.390946,2.16759),(0.39875,2.00317),(0.406555,1.91662),(0.414358,1.84987),(0.422161,1.71349),(0.429963,1.56812),(0.437765,1.65643),(0.445566,1.56459),(0.453367,1.51575),(0.461167,1.5019),(0.468966,1.54098),(0.476765,1.17737),(0.484563,1.50059),(0.49236,1.69813),(0.500157,2.00616),(0.507953,2.06435),(0.515749,2.07513),(0.523544,1.97748),(0.531339,2.00264),(0.539133,2.03843),(0.546926,2.06344),(0.554718,2.2132),(0.562511,2.32483),(0.570302,2.33467),(0.578093,2.28032),(0.585883,2.2113),(0.593672,2.1537),(0.601461,2.17244),(0.60925,2.18609),(0.617037,2.15545),(0.624824,2.15726),(0.632611,2.05623),(0.640396,2.04581),(0.648181,1.95217),(0.655966,1.94441),(0.66375,1.89155),(0.671533,1.88394),(0.679316,1.96018),(0.687097,1.87429),(0.694879,1.88617),(0.702659,1.82103),(0.710439,1.80039),(0.718219,1.81257),(0.725997,1.70694),(0.733775,1.64992),(0.741553,1.43077),(0.749329,1.40586),(0.757105,1.30714),(0.764881,1.26001),(0.772655,1.19524),(0.78043,1.12557),(0.788203,1.09229),(0.795976,1.05045),(0.803748,1.02059),(0.811519,0.97723),(0.81929,0.939279),(0.82706,0.900667),(0.834829,0.870889),(0.842598,0.82784),(0.850366,0.780731),(0.858134,0.747076),(0.8659,0.702035),(0.873666,0.665308),(0.881432,0.620493),(0.889196,0.574953),(0.89696,0.53129),(0.904723,0.491195),(0.912486,0.442125),(0.920248,0.377607),(0.928009,0.254609),(0.93577,0.151113),(0.943529,0.136912),(0.951289,0.101994),(0.959047,0.0855619),(0.966805,0.0838213),(0.974562,0.0783717),(0.982318,0.0767166),(0.990074,0.0527245),(0.997829,0.0324601),(1,0),(1.2,0))
Units: Dmnl (54)

Equation (54) is the lookup function used to find values of the nondimensional depth, d_t/d_0 or d_t' at time t, that are changed by the relative distance, s_t/S or s_t' at time t (Eq. 51), expressed as:

$$d_t' = \text{WITH LOOKUP}(s_t', [(s_{\min}', d_{\min}')\text{-}(s_{\max}', d_{\max}')], (s_0', d_0'), (s_1', d_1'), ..., (s_n', d_n')) \tag{55}$$

where $s_{\min}'$ and $s_{\max}'$ are the minimum and maximum values for the relative distance; and $d_{\min}'$ and $d_{\max}'$ are the minimum and maximum values for the nondimensional depth. Linear interpolation (Eq. 21) is used for values between the specified points, (s_i', d_i'). If $s_t' = s_i'$, the expression returns d_i' (see Section 1.2.1, Chapter 3).

APPENDIX B
Excel equations for the SPEED model

The SPEED model is an Excel spreadsheet, with the following equations:

H19 = IF(H16=0, "Ma Error", H12+H13+(H14+H15)/H16) (56)

H20 = H7-(H8+H9+H10+H11/4) (57)

H21 = IF(H19="Ma Error", "Ma Error",H19/H20) (58)

H22 = IF(H21="Ma Error", "Ma Error", IF(AND(H21<=1,H21>0),1,IF(H21>1,0,
"error"))) (59)

H25 = IF(AND(H22=1, I22=1, J22=1),"Alright", IF(AND(H22=1, I22=1, J22=0),
"Debatable", IF(AND(H22=1, I22=0, J22=0),"Critical", IF(AND(H22=0,
I22=0,J22=0), "Super-critical", "Error found")))) (60)

H26 = IF(H25="Alright", "Safety = 100%",IF(H25="Debatable", "Safety = 67%",
IF(H25="Critical", "Safety = 33%", IF(H25="Super-critical", "Safety = 0%","Please
check the input")))) (61)

I19 = IF(I16=0, "Ma Error", I12+I13+(I14+I15)/I16) (62)

I20 = I7-(I8+I9+I10+I11/4) (63)

I21 = IF(I19="Ma Error", "Ma Error",I19/I20) (64)

I22 = IF(I21="Ma Error", "Ma Error", IF(AND(I21<=1,I21>0),1,
IF(I21>1,0, "error"))) (65)

J19 = IF(J16=0, "Ma Error", J12+J13+(J14+J15)/J16) (66)

J20 = J7-(J8+J9+J10+J11/4) (67)

J21 = IF(J19="Ma Error", "Ma Error",J19/J20) (68)

J22 = IF(J21="Ma Error", "Ma Error", IF(AND(J21<=1,J21>0),1,IF(J21>1,0,
"error"))) (69)

APPENDIX C
Vensim equations for the TOP model

The TOP model is a static model written in Vensim language. Its equations with units of measurement are listed below.

$L = 50$ Units: m (70)
$S = 600$ Units: m (71)
$T = 20$ Units: Minute (72)
$Tc = 116$ Units: Minute (73)
$Td = 6$ Units: Minute (74)
$Tm = 40$ Units: Minute (75)
$Tp = 10$ Units: Minute (76)
$Tr = 1.5$ Units: Minute (77)
$Tw = 3$ Units: Minute (78)
$V = 30$ Units: m/Minute (79)
$ASET = Tc - (Tm + T / 4 + Tr + Tw)$ Units: Minute (80)
$HQ = RSET/ASET$ Units: Dmnl (81)
$RSET = Tp + Td + (S + L)/V$ Units: Minute (82)

APPENDIX D
Publication

This appendix provides the full text of the paper that reports part of the results of this study. The paper has been accepted on September 13, 2007, by Dr. Tad S. Murty, Vice-President of the Tsunami Society, for publication in *Natural Hazards*, the journal of the International Society for the Prevention and Mitigation of Natural Hazards. The original publication is available at http://dx.doi.org/10.1007/s11069-007-9183-5, and reproduced on the pages that follow, with kind permission from Springer Science and Business Media.

Nat Hazards
DOI 10.1007/s11069-007-9183-5

ORIGINAL PAPER

Method of calculating tsunami travel times in the Andaman Sea region

Monte Kietpawpan · Parichart Visuthismajarn · Charlchai Tanavud · Mark G. Robson

Received: 24 June 2007 / Accepted: 13 September 2007

Abstract A new model to calculate tsunami travel times in the Andaman Sea region has been developed. The model specifically provides more accurate travel time estimates for tsunamis propagating to Patong Beach on the west coast of Phuket, Thailand. More generally, the model provides better understanding of the influence of the accuracy and resolution of bathymetry data on the accuracy of travel time calculations. The dynamic model is based on solitary wave theory, and a lookup function is used to perform bilinear interpolation of bathymetry along the ray trajectory. The model was calibrated and verified using data from an echosounder record, tsunami photographs, satellite altimetry records, and eyewitness accounts of the tsunami on 26 December 2004. Time differences for 12 representative targets in the Andaman Sea and the Indian Ocean regions were calculated. The model demonstrated satisfactory time differences (<2 min/h), despite the use of low resolution bathymetry (ETOPO2v2). To improve accuracy, the dynamics of wave elevation and a velocity correction term must be considered, particularly for calculations in the nearshore region.

Keywords Tsunami travel time · Tsunami evacuation time · Bathymetry error · ETOPO2v2 · ETOPO5 · System dynamics

---

M. Kietpawpan (✉) · P. Visuthismajarn
Faculty of Environmental Management, Prince of Songkla University, Hat Yai,
Songkhla 90112, Thailand
e-mail: kietpawpan@yahoo.com

P. Visuthismajarn
e-mail: parichart.v@psu.ac.th

C. Tanavud
Faculty of Natural Resources, Prince of Songkla University, Hat Yai, Songkhla90112, Thailand
e-mail: charlchai.t@psu.ac.th

M. G. Robson
Environmental and Occupational Health Division, UMDNJ-School of Public Health,
and the New Jersey Agricultural Experiment Station—Rutgers University,
88 Lipman Drive, Martin Hall, New Brunswick, NJ 08901, USA
e-mail: robson@aesop.rutgers.edu

Abbreviations

CERC	Coastal Engineering Research Center
HD	Hydrographic Department
MONTE	Method of nearfield tsunami exploring
NGDC	National Geophysical Data Center
RK4	Fourth-order Runge–Kutta integration
TD	Time difference
TMD	Thai Meteorology Department

1 Introduction

There is a clear need today for accurate predictions of tsunami travel times to areas, such as Thailand, that are known to be susceptible to tsunamis. To accomplish this, people must be trained to use the most accurate models of tsunami propagation available. The accuracy of such models is principally limited by uncertainty in specification of the tsunami source, inaccuracies in bathymetry data and mapping, and possible under-resolution of the propagating wave front in the numerical simulation (Dalrymple et al. 2006). Travel time calculations to date have been rather unsuccessful, due to problems with state-of-the-art methods for propagation modeling. Whether shallow water equations or Boussinesq equations are used, the most fundamental shortcomings of most models (e.g., Holloway et al. 1985; Shokin et al. 1987; Satake 1988; Wessel 2005) are their failure to accurately represent the continuity of bathymetric profile along the ray path, the dynamics of wave elevation, and the actual speed of the first crest in shallow water. For this reason, models with coarse grid sizes fail to accurately reproduce tsunami travel times, and the use of low resolution bathymetry has often been misperceived as a major cause of the failures. To address this problem, we developed a more accurate model for predicting tsunami travel times, using a new state-of-the-art method for calculating tsunami speed.

2 Theoretical formulation

Tsunami travel time is defined here as the time it takes for the leading crest of a tsunami to travel the distance between its source and a considered target. To calculate tsunami travel times, we relied on the theoretical concepts described below.

Consider a case where a tsunami propagates from its source to the shoreline of a beach. If s is the distance traveled by the leading crest, and S is the total distance between the source and the target, the tsunami travel time, T, can be found on the graph of the function $s(t)$. The x-coordinate of the point $(t, s(t))$ can be located on the graph, provided that $s(t) = S$ and that the values of s are calculated throughout the interval $0 \leq t \leq T$ or $0 \leq s \leq S$.

In spherical coordinates, the total distance S is the length of the minor great circle arc connecting the source and the target. Thus,

$$S = R \arccos(\sin\theta_0 \sin\theta_1 + \cos\theta_0 \cos\theta_1 \cos(\lambda_0 - \lambda_1)) \tag{1}$$

where R is the Earth's radius; θ is latitudes and λ is longitudes in radians, with subscripts 0 and 1 indicating the source and the target, respectively.

The leading crest is assumed to move along the shortest great circle path or ray trajectory. This progressive motion results in the accumulation of the distance propagated by the crest, denoted by s. Thus, the distance propagated $s(t)$ to time t is given by

$$s(t) = s(t_0) + \int_{t_0}^{t} c(\tau)\ \mathrm{d}\tau \tag{2}$$

where $s(t_0)$ is the distance propagated at time 0, and $c(\tau)$ is the wave celerity at any time τ between the initial time t_0 and the current time t.

Assuming that wave celerity remains constant through out the time interval Δt, then

$$s_t = s_{t-\Delta t} + \Delta t \cdot c_t \tag{3}$$

where s_t denotes $s(t); s_{t-\Delta t}$ is the distance propagated from time 0 to the preceding time, $t - \Delta t; c_t$ is the wave celerity at time t; and Δt is a small time step.

Shallow water approximation based on the Airy wave theory is used to find c_t at time t. A tsunami propagating in the open water behaves like a sinusoidal wave with small amplitude (relative depth $<$ 0.05) and that the leading wave is the longest in a real wave train (Dalrymple et al. 2006). Therefore, the wave celerity depends only on depth, given by

$$c_t = \sqrt{g d_{t-\Delta t}} \tag{4}$$

where g is gravity acceleration, and $d_{t-\Delta t}$ is the still water level below the crest at time $t - \Delta t$.

Bilinear interpolation is then used to find the value of $d_{t-\Delta t}$:

$$d_{t-\Delta t} = d_\mathrm{a} + (d_\mathrm{b} - d_\mathrm{a})(s_{t-\Delta t} - s_\mathrm{a})/(s_\mathrm{b} - s_\mathrm{a}) \tag{5}$$

$$d_\mathrm{a} = d_\mathrm{La} + (d_\mathrm{Ua} - d_\mathrm{La})(\theta_\mathrm{a} - \theta_\mathrm{La})/(\theta_\mathrm{Ua} - \theta_\mathrm{La}) \tag{6}$$

$$d_\mathrm{b} = d_\mathrm{Lb} + (d_\mathrm{Ub} - d_\mathrm{Lb})(\theta_\mathrm{b} - \theta_\mathrm{Lb})/(\theta_\mathrm{Ub} - \theta_\mathrm{Lb}) \tag{7}$$

where d_a and d_b are the interpolated depths for the points (θ_a, λ_a) and (θ_b, λ_b) on the propagation path; s_a and s_b are the geodetic distances from the source (θ_0, λ_0) to the points (θ_a, λ_a) and (θ_b, λ_b); λ_a and λ_b are the registered longitudes ($\lambda_\mathrm{b} = \lambda_\mathrm{a} + 2$) nearest to the leading crest with $s = s_{t-\Delta t}$ and $s_\mathrm{a} < s_{t-\Delta t} < s_\mathrm{b}; d_\mathrm{La}$ and d_Lb are the registered depths for the points (θ_La, λ_a) and (θ_Lb, λ_b); θ_La and θ_Lb are the registered lower latitudes nearest to θ_a and θ_b; d_Ua and d_Ub are the registered depth for the points (θ_Ua, λ_a) and (θ_Ub, λ_b); and θ_Ua and θ_Ub are the registered upper latitudes nearest to θ_a and θ_b, respectively (Fig. 1).

As (θ_a, λ_a) and (θ_b, λ_b) are points on the great circle, it follows that

$$\begin{aligned}\theta_\mathrm{a} = \arctan((&\sin\theta_0 \cos\theta_1 \sin(\lambda_\mathrm{a} - \lambda_1)\\ &- \sin\theta_1 \cos\theta_0 \sin(\lambda_a - \lambda_0))/(\cos\theta_0 \cos\theta_1 \sin(\lambda_0 - \lambda_1)))\end{aligned} \tag{8}$$

$$\begin{aligned}\theta_\mathrm{b} = \arctan((&\sin\theta_0 \cos\theta_1 \sin(\lambda_\mathrm{b} - \lambda_1)\\ &- \sin\theta_1 \cos\theta_0 \sin(\lambda_\mathrm{b} - \lambda_0))/(\cos\theta_0 \cos\theta_1 \sin(\lambda_0 - \lambda_1)))\end{aligned} \tag{9}$$

As a tsunami moves into shallower water near the coast, it slows down, and wave height increases via conservation of energy flux, which influences wave celerity. If the bathymetric changes are so gradual as to not cause reflection, the wave height at time

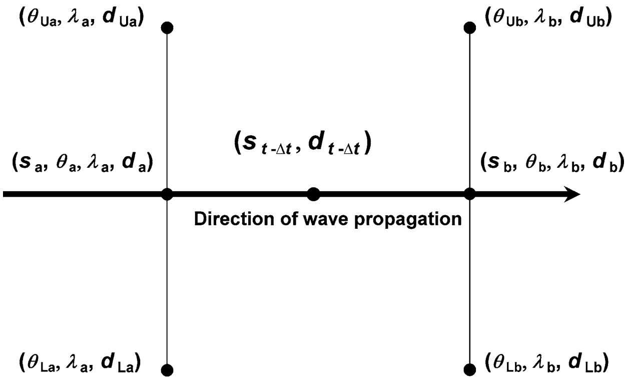

Fig. 1 Symbols used in the paper to express the bilinear interpolation of local water depth

$t - \Delta t, H(t - \Delta t)$, can be predicted by Green's law (Green 1838; Muraleedharan et al. 2006a, b):

$$H_{t-\Delta t} = H_0 (d_0 / d_{t-\Delta t})^{1/4} \tag{10}$$

where H_0 is the initial wave height, and d_0 is the still water level at the tsunami source.

Because the leading crest feels the ocean bottom at any depth (Bryant 2001), wave height varies along the ray path. Wavelength should increase and wave height should decline in deep water via conservation of energy flux, for the same reason that the wave height increases in shoaling water. This theory was confirmed by satellite altimetry observation of the 26 December 2004 tsunami (Gower 2005): the tsunami detected in the deeper Indian Ocean was greater in wavelength (400–500 km) and smaller in amplitude (0.6 m) than its initial length and height in the shallower source region. Therefore, Eq. 4 is adapted to

$$c_t = \sqrt{g(d_{t-\Delta t} + H_{t-\Delta t})} \tag{11}$$

which has been considered a good approximation of a solitary wave (CERC 1984; Sato 1996).

A tsunami does not grow infinitely, as is incorrectly predicted by Green's law. It either breaks in the surf zone or remains stable until nearly reaching the shoreline (Grawin 2005). According to Yeh et al. (1994), the leading crest of a tsunami behaves like a stable solitary wave, which is capable of maintaining its form during propagation by balancing weakly nonlinear and weakly dispersive effects. A wave breaks in shallow water when the steepness (i.e., height/length) exceeds 1/7. Tsunami waves usually do not break in shallow water, because their wavelength (L) is still a few kilometers. If it is assumed that the leading crest of most tsunamis evolves to maximum height $H_{\max}$ in shallow water and remains stable until the wave reaches the shoreline, Green's law can be modified as follows:

$$H_{t-\Delta t} = \begin{cases} H_0 (d_0 / d_{t-\Delta t})^{1/4} & \text{if } H_{t-\Delta t} < H_{\max} \\ H_{\max} & \text{if } H_{t-\Delta t} \geq H_{\max} \end{cases} \tag{12}$$

3 Model development

3.1 Model purpose

A new model of tsunami travel times, method of nearfield tsunami exploring (MONTE), was developed to more accurately calculate tsunami travel times to tsunameters in the Andaman Sea and to a community in Thailand that was hit by the tsunami of 26 December 2004. The model was also used to determine the required degree of bathymetry accuracy to ensure accurate calculation of tsunami travel times. The model focuses on the leading crest of a nearfield tsunami generated by an earthquake in the Sunda Subduction Zone and propagating along the shortest path to the populous Patong Beach on the west coast of Phuket. Other targets were included for model validation (Fig. 2).

3.2 Model conceptualization

The first step in building the model was to express the theoretical concepts described in Sect. 2 as a level-rate diagram, so that a system dynamics modeling technique could be used to solve the function of $s(t)$ over the interval $[0, T]$. Guided by the principles of systems (Forrester 1990), key theoretical concepts, consisting of parameters and variables that govern the dynamics of wave celerity along the ray trajectory, were selected as model components. The variables were further classified into level, rate, and auxiliary variables. Level variables represent where the accumulation takes place in the system. Rate variables represent what causes levels to change. Auxiliary variables represent what affects rates and can change immediately in response to changes in levels. A flow diagram clarifies how these model components are causally related (Fig. 3).

Wave celerity is the rate that increases distance propagated, which in turn increases relative distance of the leading crest, which alters local water depth and wave height, both

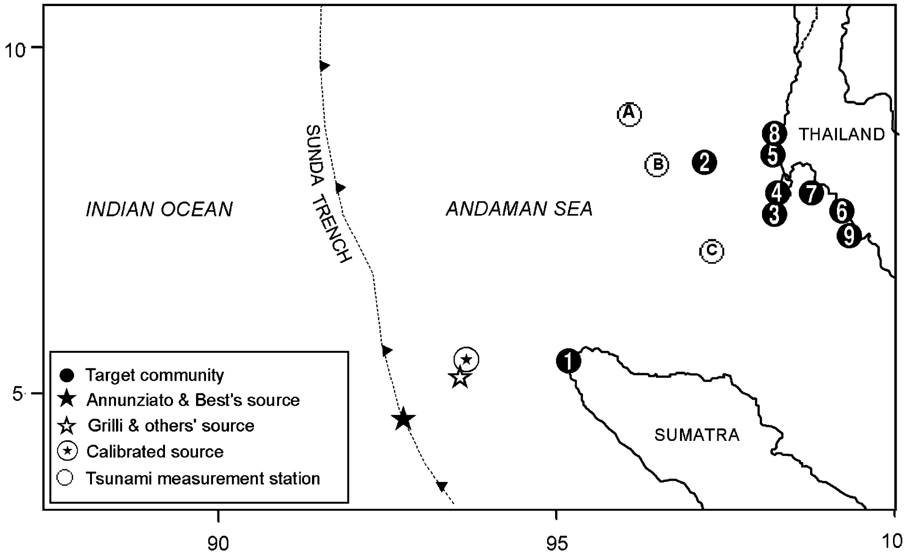

Fig. 2 Map of tsunami sources and some targets in the Andaman Sea region. Numbered locations are identified in Table 3

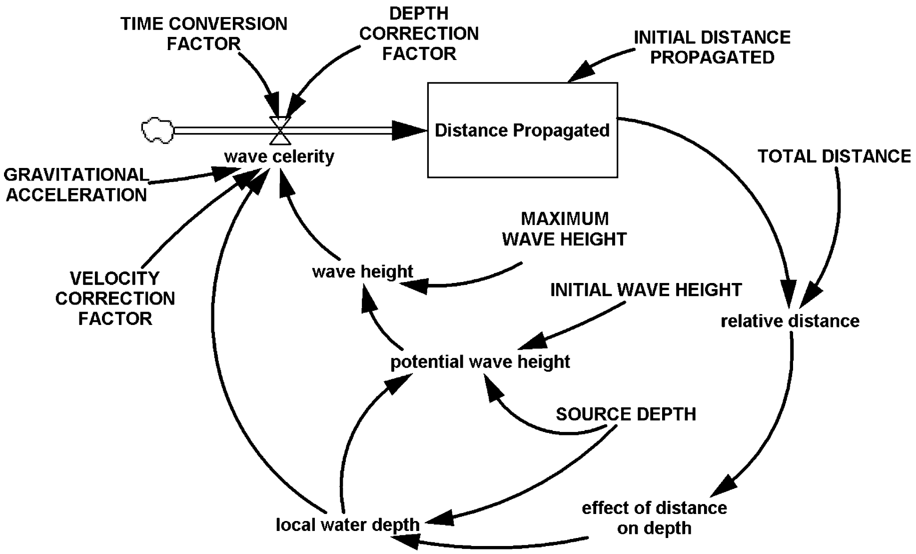

Fig. 3 Flow diagram of a tsunami travel time model

of which influence the wave celerity, which affects the level of distance propagated. This feedback relationship was considered a minimal structure necessary for calculating the travel time of a nearfield-tsunami.

3.3 Model formulation

To build the MONTE model, the flow diagram shown in Fig. 3 was entered in the Sketch Drawing Area of modeling software, Vensim (Ventana Systems 2007), and the Equation Editor tool was used to type in the equations and units of measurement (Appendix A).

Most of the parameter values used in the model were taken from reports on the 26 December 2004 tsunami (see Sect. 3.4.2). The model's tsunami source (5.458°N, 94.000°E) is a calibrated source near to the eastern border of the southern rupture zone (Fine et al. 2005; Grilli et al. 2007), far from the fault epicenter that was noted in Annunziato and Best (2005) as the tsunami source (Fig. 1). The model's target is the shoreline of Patong Beach (7.9°N, 98.276°E). The model was run on an IBM laptop computer (Pentium M, 1.5 GHz, and 248 MB RAM). The fourth-order Runge–Kutta (RK4) integrations were made with a 0.03125 min step. With the selected parameters, the model reproduced the tsunami travel time to Patong Beach with calculation error less than 2 min/h, which is the maximum acceptable error used in Shokin et al. (1987).

3.4 Model validation

The structural soundness and accuracy of the MONTE model in generating accurate predictions of tsunami travel times to both tsunameters and shorelines in the Andaman Sea region was validated using three types of tests: (i) structural tests, (ii) structurally-oriented behavior tests, and (iii) point prediction test (Forrester and Senge 1980; Sterman 2000).

3.4.1 Structural verification

To confirm that the model structure is found in the real system, we compared components and equations of the model with the available theory or relevant descriptive knowledge of tsunami dynamics. Most of the components and equations are easily recognized and have equivalent concepts in classical tsunami theory (Table 1). However, some components are uncommon.

Effect of distance on depth, E_d (Eq. 34), is the lookup function used to generate the values of local water depth in response to changes in the position of the leading crest in the ray trajectory. The relationship is specified as a table of values for the relative distance, s_t' ($s_t' = s_t/S$), and the nondimensional water depth, d_t' ($d_t' = d_t/d_0$). Linear interpolation (Eq. 5) is used for values between the specified points:

Table 1 Model structure with real system equivalents

Model components	Real system equivalents	Sources
Distance propagated	Distance traveled $s(t)$	Shokin et al. (1987)
Effect of distance on depth	Relationship between s and d	a
Potential wave height	Wave height H_2	Dean and Dalrymple (1992)
Relative distance	Nondimensional distance $s'(t)$	b
Still water depth	Still water level d	CERC (1984)
Wave celerity	Wave celerity or phase velocity C	CERC (1984)
Wave height	Wave height H	CERC (1984)
DEPTH CORRECTION FACTOR	Errors in bathymetry data ε	b
FINAL TIME	Final time of simulation t_n	b
GRAVITATIONAL ACCELERATION	Normal gravity γ	Moritz (2000)
INITIAL DISTANCE PROPAGATED	Distance propagated at time 0 $x(t_0)$	a
INITIAL TIME	Tsunami generation time t_0	b
INITIAL WAVE HEIGHT	Initial wave height H_0	b
MAXIMUM WAVE HEIGHT	Maximum stable wave height H_max	b
SOURCE DEPTH	Still water level at tsunami source d_0	Grilli et al. (1997)
TIME CONVERSION FACTOR	60 s of a minute	a
TIME STEP	Temporal step Δt	Shokin et al. (1987)
TOTAL DISTANCE	Geodetic distance $R\phi$	Banerjee (2005)
VELOCITY CORRECTION FACTOR	Correction terms to the speed of the wave	a
Eq. 28	Eq. 3	b
Eq. 29	$d_t = d_0 \cdot d_t' = d_0(d_t/d_0)$	a
Eq. 30	$s' = s_t/S$	a
Eq. 31	Eq. 10	Green (1838)
Eq. 32	Eq. 15	CERC (1984) and Grilli (1997)
Eq. 33	Eq. 12	Yeh et al. (1994)
Eq. 34	Eq. 14	a

[a] Component that is not common and needs to be explained

[b] Easily recognized component

$$E_{\mathrm{d}} = \left(\frac{s_{t_0}}{S}, \frac{d_{t_0}}{d_0}\right), \left(\frac{s_{t_0+\Delta t}}{S}, \frac{d_{t_0+\Delta t}}{d_0}\right), \left(\frac{s_{t_0+2\Delta t}}{S}, \frac{d_{t_0+2\Delta t}}{d_0}\right), \ldots, \left(\frac{s_{t_0+n\Delta t}}{S}, \frac{d_{t_0+n\Delta t}}{d_0}\right) \quad (13)$$

which is equivalent to the spatial expression:

$$E_{\mathrm{d}} = \left(\frac{s_{\lambda_0}}{S}, \frac{d_{\lambda_0}}{d_0}\right), \left(\frac{s_{\lambda_0+2}}{S}, \frac{d_{\lambda_0+4}}{d_0}\right), \left(\frac{s_{\lambda_0+6}}{S}, \frac{d_{\lambda_0+6}}{d_0}\right), \ldots, \left(\frac{s_{\lambda_1}}{S}, \frac{d_{\lambda_1}}{d_0}\right) \quad (14)$$

where $n = T/\Delta t$; s is the distance propagated with subscript $\lambda_0 + i$ indicating longitudes of points along the ray trajectory, which are $2'$ apart (i = 0, 2, 4,..., j); and $\lambda_1 = \lambda_0 + j$. If $s_t/S = s'_t$ (Eq. 31), the expression returns $d'_t = d_t/d_0$. The value of d' at any relative distance s' is precomputed with linear interpolation (Eqs. 6 and 7) from ETOPO2v2.

DEPTH CORRECTION FACTOR F_{d} (Eq. 16) denotes the degree of error in the bathymetry data used in the model. If $F_{\mathrm{d}} = 1$, the data are treated as error-free. If $F_{\mathrm{d}} < 1$, the data over-predict the actual bathymetry, i.e., overestimate depth. If $F_{\mathrm{d}} > 1$, they under-predict the actual bathymetry and underestimate depth.

TIME CONVERSION FACTOR F_{t} (Eq. 24) converts the unit of wave celerity from m/s to m/min.

VELOCITY CORRECTION FACTOR F_{v} (Eq. 27) is a multiplier that corrects the speed of the wave in the high crest region, where low-order theories have been found to under-predict celerity by as much as 50% (Grilli 1997). In the model, we assume that solitary wave theory under-predicted the speed of the first crest by 38% (F_{v} = 1.6).

3.4.2 *Parameter verification*

Parameter verification determined whether parameter values used in the MONTE model fall within a plausible range of the actual values measured for the tsunami of 26 December 2004. All the assumed parameter values are consistent with those of the real event (Table 2).

3.4.3 *Reality check*

The reality check confirmed that the model exhibits appropriate behavior when selected parameters are assigned extreme values or values for which the logical consequences are known. The MONTE model behaves plausibly under the following extreme and non-extreme conditions:

- If wave celerity becomes zero, the wave stops propagating.
- If the earth lacks gravity, the crest does not propagate.
- If there is no initial disturbance, then no tsunami is observed.
- When the crest reaches the shoreline, it is 6 m in height.
- When the crest reaches the shoreline, the local water depth is zero.
- When the distance propagated is equal to zero, the water depth is equal to the depth at the source.
- In a sea of constant depth, the simulated travel time is equal to the travel time derived analytically (total distance/constant wave celerity).
- The wave height decays in the Indian Ocean as detected by JASON-1 observation.

Table 2 Model parameter values with a plausible range of actual values

Parameters (units)	Assigned values	Actual values	Sources
d_0 (m)	527	[453, 553]	NGDC (2007)
d_t (m)	ETOPO2v2	≈ETOPO2v2	NGDC (2007)
F_d (Dmnl)	1	≥ 1	Johannesson and Mitson (1983)
F_t (s/min)	60	60	[a]
F_v (Dmnl)	1.6	(1, 2]	Grilli (1997)
g (m/s^2)	9.8	[9.78, 9.83]	Moritz (2000)
H_0 (m)	1.5	[1.5, 10]	Bilham (2005) and Halif and Sabki (2005)
H_{max} (m)	6	[5, 6]	Kawata et al. (2005)
R (m)	6371000	(6371000, 63710008]	Moritz (2000)
$s(t_0)$ (min)	0	0	[a]
S (m)	544710	≈544710	Banerjee (2005)
t_0 (min)	0	0	[a]
t_n (min)	120	>115	[a]
Δt (min)	0.03125	0	Bryant (2001)
λ_0 (radians)	1.6406095	[1.650, 1.627]	Grilli et al. (2007)
λ_1 (radians)	1.715239776	1.715239776	Grilli et al. (2007)
θ_0 (radians)	0.0953	[0.0668, 0.1293]	Grilli et al. (2007)
θ_1 (radians)	0.13788	0.13788	Grilli et al. (2007)

[a] Easily assigned value

3.4.4 Boundary adequacy

The boundary adequacy test confirmed that the model incorporates all of the major concepts and relationships for calculating tsunami travel times in the Andaman Sea region. Airy wave theory (Eq. 4) and solitary wave theory (Eq. 11) over-predicted the travel time to Patong Beach by as much as 10% (time difference = 6 min/h), implying that such low-order theories under-predicted the speed of the first crest, as already noted in Grilli (1997). To solve this problem, the boundary of the model was extended by including a correction term, the velocity correction factor that increased the speed of the crest in the shallow water region:

$$c_t = \begin{cases} \sqrt{g(d_{t-\Delta t} + H_{t-\Delta t})} & \text{if } d_{t-\Delta t} > 50 \text{ m} \\ F_v\sqrt{g(d_{t-\Delta t} + H_{t-\Delta t})} & \text{if } d_{t-\Delta t} \leq 50 \text{ m} \end{cases} \tag{15}$$

The corrected model provides better predictions for all the considered targets (see Sect. 3.4.6).

3.4.5 Syntax accuracy and dimensional consistency

The model syntax and measurement units were checked using the automated analysis functions provided by the Vensim simulation environment. The model contains neither syntax errors nor dimensional errors. In addition, all the units are easily recognized and have realistic meanings. Note that the unit ‘Dmnl’ stands for dimensionless, which is the unit of a ratio.

3.4.6 Behavior reproduction

Travel times for the first crest that propagated from the southern source region of the 26 December 2004 tsunami to some targets in the Andaman Sea region calculated using the MONTE model were compared to the observed travel times from four information sources: an echcosounder record, tsunami photographs, satellite altimetry records, and eyewitness accounts. Measurements from tide gauge stations on the coast of Thailand were not used because of inadequate resolution (Fine et al. 2005); it is difficult to accurately determine times from these low-speed analog paper records (Rabinovich and Thomson 2007), as the times recorded on some of the sheets are imprecise (Tsuji et al. 2006). Deviations between the calculated and observed travel times proved to be satisfactorily small for most of the targets, including those in the open sea and in coastal areas (Table 3). In most cases, the time differences did not exceed 3%, or 2 min/h of wave propagation. The calculated travel times suggest that the first crest propagated from the border of the southern source areas, extending northward from the island of Sumatra, not from the fault epicenter as speculated in Annunziato and Best (2005).

The differences between the calculated and observed travel times were small for all the targets except Phi Phi Don (Table 3), where the nearshore bathymetry based on ETOPO2v2 contains a large error. Compared with a Royal Thai Navy's bathymetric chart (HD 2004), the ETOPO2v2 data set under-predicted the average water depth along the last 94 km of the ray path to Phi Phi Don by as much as 57%. Replacement of ETOPO2v2 bathymetry data for that region with the more accurate Navy data resulted in a highly improved prediction (time difference = 1.2 min/h).

Of the sources of travel times observed in the Andaman Sea region for the 26 December 2004 tsunami, the echosounder record made from the Belgian yacht, Mercator (Rabinovich and Thomson 2007), and the tsunami photographs taken in Khao Lak and Koh Lanta (Heinrich Grosskopf 2007, private communication) are considered the most reliable (Fine et al. 2005). Therefore, data from these sources were used to calibrate the model by fine tuning the velocity correction factor ($F_v = 1.6$). The model was then used to predict travel times to other targets for which only eyewitness accounts are available. All model results agreed well with the observed travel times: the time differences were all under 2 min/h.

Table 3 Tsunami travel times and time differences for some targets of the 26 December 2004 tsunami

No.	Target	Coordinates	Tsunami travel time		TD[¶]
			Observed	Computed	
1	Banda Aceh	5.458°N, 95.247°E	31 min[a]	30 min	1.9
2	Koh Similan	8.498°N, 97.627°E	1 h 37 min[b]	1 h 38 min	−0.6
3	Mercator	7.750°N, 98.280°E	1 h 55 min[c]	1 h 55 min	0.1
4	Patong Beach	7.900°N, 98.276°E	1 h 56 min[d]	1 h 56 min	0.1
5	Phi Phi Don	7.739°N, 98.772°E	2 h 21 min[e]	2 h 53 min	−13.6*
6	Khao Lak	8.857°N, 98.268°E	2 h 28 min[f]	2 h 24 min	1.6
7	Koh Lanta	7.534°N, 99.031°E	2 h 34 min[g]	2 h 36 min	−0.7
8	Koh Phra Thong	9.136°N, 98.266°E	2 h 41 min[h]	2 h 41 min	0.1
9	Morakot Cave	7.402°N, 99.230°E	3 h[i]	2 h 59 min	0.2

[a] SAN (2005); [b] Gray (2005); [c] Fine et al. (2005); [d] Papadopoulos et al. (2006); [e] Bowman (2005); [f] Thomson (2005); [g] Freund (2005); [h] Raderstorf (2004); [i] Emery (2005); [¶] Time difference (min/h) = $60(T_o - T_c)/T_o$, where T_o is the observed tsunami travel time and T_c is the calculated tsunami travel time. * Significant error: $|TD| > 2$ min/h

3.4.7 Family member test

The family member test determined whether or not the MONTE model is applicable to geographic areas other than the Andaman Sea. The calculations predicted travel times to three representative targets in the Indian Ocean region, based on the same assumptions noted earlier, except that the tsunami sources were located near the western, rather than the eastern, border of the southern rapture zone, about 100 km from the tsunami source used for targets in the Andaman Sea region. The model reproduced the travel time with satisfactory accuracy (Table 4). Thus, the model is general enough to provide accurate calculations of tsunami travel times to tsunameters and target communities in the Indian Ocean, as well as in the Andaman Sea region.

3.4.8 Sensitivity test

The sensitivity test determined whether the predictions of the MONTE model change more than 2 min/h when the model's assumptions and parameters are varied over the plausible range of uncertainty, including maximum wave height, gravitational acceleration, initial wave height, initial water depth, time steps, integration methods (Euler and RK4), bathymetry data sets (ETOPO5 and ETOPO2v2), bathymetry resolutions (4–10 min), and bathymetry errors (1–15%). Predicted tsunami travel times to Patong Beach were relatively insensitive to values of maximum wave height, gravity, initial wave height, initial water depth, and time steps (Table 5). The Euler and RK4 methods did not give significantly different results. In all cases, the time differences were well below 2 min/h. Thus, the model is capable of generating a plausible prediction, even when the exact values of these parameters are unknown.

Predictions of the MONTE model were sensitive to accuracy of bathymetry data. ETOPO5 (NGDC 2006) under-estimated the nearshore bathymetry of Patong Beach by as much as 23%, causing the tsunami travel time to the beach to be overestimated by as much as 5.25 min (2.7 min/h). The largest part of this calculation error (5.68 min) was due to the underestimated

Table 4 Tsunami travel times and time differences for targets in the Indian Ocean

No.	Target	Coordinates	Tsunami travel time		TD
			Observed	Computed	
1	Jason-1	03.01°S, 84.68°E	1 h 55 min[a]	1 hr 56 min	−0.5
2	Topex/Poseidon	02.80°S, 83.34°E	2 h 02 min[a]	2 h 04 min	−1.0
3	Chennai	13.10°S, 80.32°E	2 h 45 min[a]	2 h 49 min	−1.4

[a] Fine et al. (2005)

Table 5 Sensitivity to some parameters of tsunami travel times predicted to Patong Beach

Parameters	Assigned values	TD[a]
Acceleration due to gravity (m/s^2)	[9.7, 10]	[−0.30, 0.61]
Time step (s)	[0.4, 60]	[−0.01, 0.47]
Initial wave height (m)	[0.6, 7]	[−0.34, 0.53]
Maximum wave height (m)	[2, 8]	[−0.22, 0.01]
Initial water depth (m)	[100, 4000]	[−0.19, 0.32]

[a] Time difference (min/h) = $60(T_b - T_s)/T_b$, where T_b is the tsunami travel time of the best estimate run (115.91 min) and T_s is that of a sensitivity run

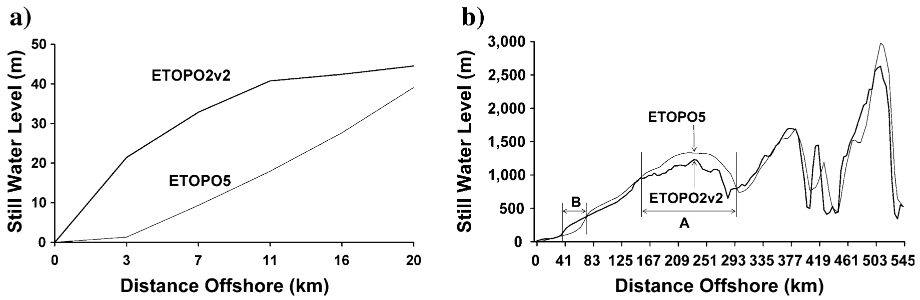

Fig. 4 Two bathymetry profiles along the ray trajectory to Patong Beach, based on the ETOPO5 and ETOPO2v2 data sets. (**a**) ETOPO5 error in nearshore region. (**b**) Major regions (A and B) of ETOPO5 error in offshore region

bathymetry (53.7%) in the last 20 km of tsunami propagation (Fig. 4a). Smaller time errors (2.5 and −3.56 min) were found in regions A and B (Fig. 4b), where the average ETOPO5 errors in water along the ray trajectories were about 14.1 and −30.7%, respectively (Table 6).

Unlike accuracy of the bathymetry data, bathymetry resolution had little effect on predictions of travel times to Patong Beach and other targets in the Andaman Sea region. To determine this sensitivity, different bathymetry data sets were prepared from ETOPO2v2 (NGDC 2007) by removing points along the ray trajectory to produce lower resolutions (4′–10′). Tsunami travel times based on those datasets showed negligible time differences (Table 6). Thus, calculation error in model predictions is caused primarily by inaccuracy in bathymetry derived from ETOPO5, not by the low resolution of this data set. More accurate bathymetry data sets with even lower resolutions (e.g., 6′–10′), would provide better predictions than ETOPO5 (Table 6). Bathymetry data accurate to 94% (error $\leq$ 6%) are necessary to keep the time difference under 2 min/h.

Because the ETOPO2v2 data set is most reliable in the open sea ($\geq$200 km offshore), that region was treated as error-free, and only the nearshore bathymetry data (<200 km offshore)

Table 6 Time differences for some levels of bathymetry resolution and error in nearshore regions

Bathymetry data	TD (min/h)								
	Targets[a]								
	1	2	3	4	5	6	7	8	9
Resolution (min)									
4	0.74	0.02	0.21	−0.71	0.68	0.10	0.03	−0.63	0.03
6	0.74	0.21	0.22	−0.65	0.29	0.52	0.10	0.03	0.12
8	0.60	−0.05	0.27	−1.03	0.13	0.42	0.26	−0.58	0.05
10	1.40	0.31	−0.43	1.44	−1.22	0.29	1.71	0.03	0.06
Error (%)									
1	0.30	0.31	0.29	0.29	0.28	0.29	0.55	0.29	0.30
6	1.69	1.73	1.67	1.66	1.62	1.71	1.95	1.68	1.73
7	1.96	1.99	1.95	1.92	1.88	1.97	2.23*	1.96	2.00*
8	2.23*	2.27*	2.21*	2.18*	2.13*	2.24*	2.49*	2.22*	2.28*

* Significantly sensitive, $|TD| \geq 2$ min/h

[a] 1 = Chennai; 2 = Jason-1; 3 = Khao Lak; 4 = Koh Lanta; 5 = Koh Lanta; 6 = Koh Phra Thong; 7 = Koh Similan; 8 = Patong Beach; 9 = Topex/Poseidon

Table 7 Time differences under some degrees of resolution and accuracy of nearshore bathymetry

Bathymetry error (%)	TD[a] (min/h)								
	Distance nearshore (km)								
	200	150	100	50	25	20	15	10	5
1	0.15	0.13	0.10	0.01	0.03	0.03	0.05	0.02	0.00
5	0.73	0.61	0.49	0.32	0.16	0.13	0.13	0.06	0.03
10	1.39	1.20	0.94	0.60	0.29	0.26	0.21	0.13	0.06
14	1.89	1.62	1.28	0.83	0.40	0.34	0.26	0.18	0.10
15	2.01*	1.71	1.36	0.87	0.44	0.36	0.29	0.19	0.10

[a] Time difference (min/h) = $60(T_b - T_s)/T_b$, where T_b is the tsunami travel time of the best estimate run (115.91 min) and T_s is that of a sensitivity run. * Significant sensitivity, $|TD| \geq 2$ min/h

were corrected by setting the depth correction factor as between 1.01 and 1.15. Nearshore bathymetry data accurate to 86% were adequate to keep the time difference under 3% (Table 7). Even lower levels of accuracy (14–43% error) would be adequate for use in the model if the satellite altimatry works best in deep water (≥200 m) as noted in Sloss (2005), making ETOPO2v2 reliable in nearshore areas (≥45 km off Patong Beach), as well as in the open sea.

Based on all the validity tests, the MONTE model meets the following conditions:

- Every element and relationship in the model has identifiable real world meanings and is consistent with available observations.
- When the model is simulated under extreme conditions, the model system's operation is reasonable, i.e., impossible behavior modes do not occur.
- The model exhibits behavior that was observed in the real system.
- The model predictions are robust under a plausible range of bathymetry error and resolution in shallow water.

Hence, we believe that the model is adequate for generating highly accurate predictions of tsunami travel times to tsunameters and many target communities in the Andaman Sea region. The model is not intended for application to the Indian Ocean, for which travel time atlases have already been published (Barman et al. 2006; Kumar et al. 2006).

4 Conclusions

The MONTE model provides a powerful tool for tsunami evacuation planning in the Andaman Sea region, because it predicts the tsunami travel time to considered targets (tsunameter/target community) with satisfactory accuracy (time difference < 2 min/h). The model is robust under a plausible range of all parameters, making it reliable even when the exact values of the parameters are not known. For reliable prediction, the model requires nearshore bathymetry be accurate to at least 57% of actual water depth, provided that ETOPO2v2 is accurate in deep water (>200 m). A more detailed bathymetry data set ($<2'$) is not needed to keep the time difference under the acceptable limit. ETOPO5 should not be used for travel time predictions to Patong Beach because the data set contains a large bathymetry error in the nearshore region, causing calculation error above 2 min/h. Future research should use the MONTE model to evaluate the effectiveness of the tsunami warning system and evacuation plans for post-tsunami communities in the Andaman Sea region (see Appendix B).

Acknowledgements This work was funded by the World Vision Foundation of Thailand. We are particularly grateful for extensive reviewer comments, which substantially improved the paper. We also thank Professor Tad S. Murty and Jinsong Xie for their suggestions for improving the model.

Appendix A: Vensim equations for the MONTE Model

DEPTH CORRECTION FACTOR = 1 (Dmnl) (16)

FINAL TIME = 120 (Minute) (17)

GRAVITATIONAL ACCELERATION = 9.8 (m/(s*s)) (18)

INITIAL DISTANCE PROPAGATED = 0 (m) (19)

INITIAL TIME = 0 (Minute) (20)

INITIAL WAVE HEIGHT = 1.5 (m) (21)

MAXIMUM WAVE HEIGHT = 6 (m) (22)

SOURCE DEPTH = 527 (m) (23)

TIME CONVERSION FACTOR = 60 (s/Minute) (24)

TIME STEP = 0.03125 (Minute) (25)

TOTAL DISTANCE = 544710 (m) (26)

VELOCITY CORRECTION FACTOR = 1.6 (Dmnl) (27)

Distance propagated = INTEG(wave celerity, INITIAL DISTANCE PROPAGATED) (m) (28)

Local water depth = (effect of distance on depth * SOURCE DEPTH) (m) (29)

Potential wave height = INITIAL WAVE HEIGHT * SQRT(SQRT(SOURCE DEPTH/local water depth)) (m) (30)

Relative distance = Distance propagated/TOTAL DISTANCE (Dmnl) (31)

Wave celerity = IF THEN ELSE (local water depth > 50,
SQRT(GRAVITATIONAL ACCELERATION * (wave height
+ (local water depth * DEPTH CORRECTION FACTOR)))
* TIME CONVERSION FACTOR, VELOCITY CORRECTION FACTOR
* SQRT (GRAVITATIONAL ACCELERATION * (wave height
+ (local water depth * DEPTH CORRECTION FACTOR)))
* TIME CONVERSION FACTOR) (m/min) (32)

Wave height = MIN (potential wave height, MAXIMUM WAVE HEIGHT) (m) (33)

$$\text{Effect of distance on depth} = \text{WITH LOOKUP(relative distance,}([(0,0)(1.2,5.04357)], (0,1), (0.00783193, 1.0541), (0.0156634, 0.636126), (0.0234943, 0.804125), (0.0313247, 1.81906), (0.0391546, 3.88361), (0.046984, 4.47011), (0.0548129, 4.62955), (0.0626412, 5.04357), (0.0704691, 4.93504), (0.0782964, 4.83528), (0.0861232, 4.23365), (0.0939495, 4.36503), (0.101775, 3.84451), (0.109601, 3.88547), (0.117425, 3.55443), (0.125249, 3.33724), (0.133073, 3.04497), (0.140896, 2.92535), (0.148719, 2.72369), (0.156541, 2.33085), (0.164362, 2.45544), (0.172183, 1.81986), (0.180004, 0.345365), (0.187824, 1.06789), (0.195643, 0.967627), (0.203462, 0.749606), (0.21128, 0.803046), (0.219098, 0.973205), (0.226915, 2.47862), (0.234732, 2.96307), (0.242548, 2.52339), (0.250363, 1.65518), (0.258178, 0.307644), (0.265993, 1.63057), (0.273806, 1.95526), (0.28162, 2.81282), (0.289432, 3.17195), (0.297245, 3.22311), (0.305056, 3.19811), (0.312867, 3.2703), (0.320678, 3.11306), (0.328487, 3.05779), (0.336297, 2.79868), (0.344106, 2.79721), (0.351914, 2.63188), (0.359721, 2.45669), (0.367528, 2.41399), (0.375335, 2.48735), (0.383141, 2.38617), (0.390946, 2.16759), (0.39875, 2.00317), (0.406555, 1.91662), (0.414358, 1.84987), (0.422161, 1.71349), (0.429963, 1.56812), (0.437765, 1.65643), (0.445566, 1.56459), (0.453367, 1.51575), (0.461167, 1.5019), (0.468966, 1.54098), (0.476765, 1.17737), (0.484563, 1.50059), (0.49236, 1.69813), (0.500157, 2.00616), (0.507953, 2.06435), (0.515749, 2.07513), (0.523544, 1.97748), (0.531339, 2.00264), (0.539133, 2.03843), (0.546926, 2.06344), (0.554718, 2.2132), (0.562511, 2.32483), (0.570302, 2.33467), (0.578093, 2.28032), (0.585883, 2.2113), (0.593672, 2.1537), (0.601461, 2.17244), (0.60925, 2.18609), (0.617037, 2.15545), (0.624824, 2.15726), (0.632611, 2.05623), (0.640396, 2.04581), (0.648181, 1.95217), (0.655966, 1.94441), (0.66375, 1.89155), (0.671533, 1.88394), (0.679316, 1.96018), (0.687097, 1.87429), (0.694879, 1.88617), (0.702659, 1.82103), (0.710439, 1.80039), (0.718219, 1.81257), (0.725997, 1.70694), (0.733775, 1.64992), (0.741553, 1.43077), (0.749329, 1.40586), (0.757105, 1.30714), (0.764881, 1.26001), (0.772655, 1.19524), (0.78043, 1.12557), (0.788203, 1.09229), (0.795976, 1.05045), (0.803748, 1.02059), (0.811519, 0.97723), (0.81929, 0.939279), (0.82706, 0.900667), (0.834829, 0.870889), (0.842598, 0.82784), (0.850366, 0.780731), (0.858134, 0.747076), (0.8659, 0.702035), (0.873666, 0.665308), (0.881432, 0.620493), (0.889196, 0.574953), (0.89696, 0.53129), (0.904723, 0.491195), (0.912486, 0.442125), (0.920248, 0.377607), (0.928009, 0.254609), (0.93577, 0.151113), (0.943529, 0.136912), (0.951289, 0.101994), (0.959047, 0.0855619), (0.966805, 0.0838213), (0.974562, 0.0783717), (0.982318, 0.0767166), (0.990074, 0.0527245), (0.997829, 0.0324601), (1,0), (1.2,0)) \quad \text{(Dmnl)} \tag{34}$$

Equation (34) is the lookup function used to find values of the nondimensional depth, d_t/d_0 or $d'_t d_t$ at time t, that are changed by the relative distance, s_t/S or s'_t at time t (Eq. 31), expressed as:

$$d'_t = \text{WITH LOOKUP}(s'_t, [(s'_{\min}, d'_{\min}) - (s'_{\max}, d'_{\max})], (s'_0, d'_0), (s'_1, d'_1), \ldots, (s'_n, d'_n)) \tag{35}$$

where s'_{min} and s'_{max} are the minimum and maximum values for the relative distance; and d'_{min} and d'_{max} are the minimum and maximum values for the nondimensional depth. Linear interpolation (Eq. 5) is used for values between the specified points (s'_t,d'_t). If $s'_t = s'_t$, the expression returnsd'_i (see Sect. 3.4.1).

Appendix B: an example of application

Problem: An earthquake generates a tsunami in the Andaman Sea similar to the 26 December 2004 event (H_0 = 1.5 m; H_{max} = 6 m; λ_0 = 5.458°N; θ_0 = 94.0°E; and T = 45 min). What safe evacuation time is available in Patong Beach (7.9°N, 98.276°E), where 2 min is needed to send a signal to the warning siren-towers on the beach (Johnstone 2005)?

Safe evacuation time predicted by the MONTE model: The tsunami is detected by three tsunameters (Fig. 2A–C). Based on Titov et al. (2001), the available safe evacuation time ($\mathrm{ASET_i}$) based on to tsunameter i is given by

$$\mathrm{ASET_i} = \mathrm{T_C} - (\mathrm{T_{Mi}} + \mathrm{T}/4 + \mathrm{T_W}) \tag{36}$$

where $\mathrm{T_C}$ is the tsunami travel time to a target community, $\mathrm{T_{Mi}}$ is the tsunami travel time to a tsunameter i, T is the period of the first tsunami wave, and $\mathrm{T_W}$ is the time required to issue the warning, The MONTE model predicts that T_{C} = 116 min, T_{MA} = 54 min, T_{MB} = 51, and T_{MC} = 71 min (Fig. 5). Therefore, $\mathrm{ASET_A}$ = 51 min, $\mathrm{ASET_B}$ = 52 min, and $\mathrm{ASET_C}$ = 32 min.

Thus, people in Patong Beach have as much as 52 min, and at least 32 min (if the first two tsunameters (A and B) fail to send waveform data), to evacuate to safe areas prior to arrival of the first tsunami. If further research shows that most vulnerable evacuees (e.g., elderly pedestrians) would take less than 32 min to reach safety, the warning system proposed in TMD (2006) would be deemed sufficiently effective. If more than 32 min are required, plans for faster evacuation would be necessary.

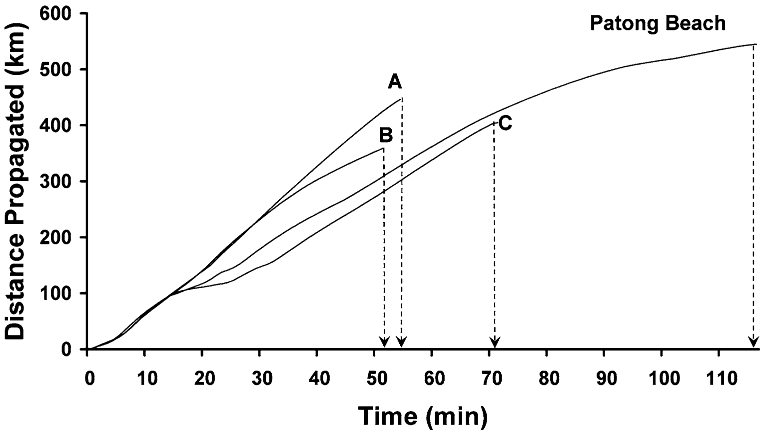

Fig. 5 Output graph of the MONTE model

References

Annunziato A, Best C (2005) The tsunami event analyses and models. Joint Research Center, European Commission. http://tsunami.jrc.it/model/simulation.pdf. Cited 25 Nov. 2005

Banerjee S (2005) On geodetic distance computations in spatial modeling. Biometrics 61:617–625

Barman R, Kumar BP, Pandey PC, Dube SK (2006) Tsunami travel time prediction using neural networks. Geophys Res Lett 33(16)

Bilham R (2005) A flying start, then a slow slip. Science 308:1126–1127

Bowman N (2005) Naomi's story. http://www.tsunamistories.net/ViewStory.aspx?StoryID=41a8fc79-9dad-4493-8765-6346b603a72e. Cited 17 May 2007

Bryant E (2001) Tsunami: the underrated hazard. Cambridge University Press, Cambridge

CERC (Coastal Engineering Research Center) (1984) Shore protection manual. US Army Engineer Waterways Experiment Station, Vicksburg

Dalrymple RA, Grilli ST, Kirby JT (2006) Tsunami and challenges for accurate modeling. Oceanography 19(1):142–151

Dean RG, Dalrymple RA (1992) Water wave mechanics for engineers and scientists. World Scientific Publishing, Singapore

Emery S (2005) Your experiences of Asian disaster. http://www.news.bbc.co.uk/1/hi/talking-point/4126255.htm. Cited 15 May 2007

Fine VF, Rabinovich AB, Thomson RE (2005) The dual source region for the 2004 Sumatra tsunami, Geophys Res Lett 32:L16602. doi:10.1029/2005GL023521

Forrester JW, Senge PM (1980) Tests for building confidence in system dynamics models. In: Legasto AJ, Forrester JW, Lyneis J (eds) TIMS studies in the management sciences, vol 14. North Holland Press, New York, pp 209–228

Forrester JW (1990) Principles of systems. Productivity Press, Portland

Freund P (2005) Khlong Nin Beach—Report & Tsunami Photo—Peter Freund. http://www.radarheinrich.de/wbblite/thread.php?threadid=1794. Cited 15 May 2007

Gower J (2005) Jason 1 detects the 26 December 2004 tsunami. Eos Trans. 86(4):37

Grawin A (2005) Tsunami photos. http://www.kohjumonline.com/grawin. Cited 20 May 2007

Gray J (2005) Tsunami media kit. http://www.johngray-seacanoe.com/pdf/Tsunami-Media-Kit.pdf. Cited 15 May 2007

Green G (1838) On the motion of waves in a variable canal of small depth and width. Trans Camb Philos Soc 6:457–462

Grilli ST (1997) Fully nonlinear potential flow models used for long wave runup prediction. In: Yeh H, Liu P, Synolakis C (eds) Long-wave runup models. World Scientific Publishing, Singapore, pp 116–180

Grilli ST, Svenden IA, Subramanya R (1997) Breaking criterion and characteristics for solitary waves. J Waterw Port Coast Ocean Eng 123(3):102–112

Grilli ST, Ioualalen M, Asavanant J, Shi F, Kirby JT, Watts P (2007) Source constraints and model simulation of the December 26, 2004 Indian Ocean Tsunami. J Waterw Port Coast Ocean Eng 133(6):414–428

Grosskopf H (2007) Personal e-mail communication to M. Kietpawpan on 20 May 2007

Halif MNA, Sabki SN (2005) The physics of tsunami: basic understanding of the Indian Ocean disaster. Am J Appl Sci 2(8):1187–1192

HD (Hydrographic Department) (2004) Bathymetry chart no. 308: Phuket to Kantang. Royal Thai Navy, Bangkok, 10260

Holloway G, Murty T, Fok E (1985) Effects of bathymetric roughness upon tsunami travel time. Sci Tsunami Hazards 4(3):165–172

Johannesson KA, Mitson RB (1983) Fisheries acoustics: a practical manual for aquatic biomass estimation. FAO fisheries technical report 240. Food and Agriculture Organization of the United Nations, Rome. http://www.fao.org/docrep/X5818E/x5818e0a.htm. Cited 17 Dec. 2006

Johnstone A (2005) How the new tsunami warning system works. http://www.phuketgazette.net/tsunami/#t2. Cited 20 May 2007

Kawata Y, Tsuji Y, Sugimoto Y, Matsutomi H, Okamura Y, Hayashi I, Kayane H, Tanioka Y, Fujima K, Maki N, Koshimura S (2005) Comprehensive analysis of the damage and its impact on coastal zones by the 2004 Indian Ocean tsunami disaster. http://www.tsunami.civil.tohoku.ac.jp/sumatra2004/report.html. Cited 15 May 2007

Kumar BP, Kumar RR, Dube SK, Murty T, Gangopadhyay A, Chaudhuri A, Rao AD (2006) Tsunami travel time computation and skill assessment for the 26 December 2004 event in the Indian Ocean. Coast Eng J 48(2):1–20

Moritz H (2000) Geodetic reference system 1980. J Geod 74(1):128–133

Muraleedharan G, Shina M, Rao AD, Murty TS (2006a) Statistical simulation of Boxing Day tsunami of the Indian Ocean and a predictive equation for beach run-up heights based on work–energy theorem. Mar Geod 29(3):223–231

Muraleedharan G, Rao AD, Murty TS, Sinha M (2006b) Validation of tsunami beach run-up height predictive model based on work–energy theorem. In: Aswathanarayana U, Nirupama N (eds) The Indian Ocean tsunami. Taylor and Francis, Netherlands, pp 131–142

NGDC (National Geophysical Data Center) (2006) ETOPO5 5-minute girdded elevation data. http://www.ndgc.noaa.gov/mgg/global/etopo5.html. Cited 22 May 2006

NGDC (2007) 2-Minute girdded global relief data (ETOPO2v2) June, 2006. http://www.ndgc.noaa.gov/mgg/fiers/06mgg01.html. Cited 27 March 2007

Papadopoulos GA, Caputo R, McAdoo B, Pavlides S, Karastathis V, Fokaefs A, Orfanogiannak K, Valkaniotis S (2006) The large tsunami of 26 December 2004: field observations and eyewitnesses accounts from Sri Lanka, Maldives Is. and Thailand. Earth Planets Space 58:233–241

Rabinovich AB, Thomson RE (2007) The 26 December 2004 Sumatra tsunami: analysis of tide gauge data from the world ocean Part 1 Indian Ocean and South Africa. Pure Appl Geophys 164(2007):261–308

Raderstorf S (2004) Raderstorf world wide adventure: alive and well in Bangkok. http://www.raderstorfwwablogspot.com/2004/alive-and-well-in-bangkok.html. Cited 15 May 2007

SAN (Save Andaman Network) (2005) Ker Kon Andaman Ker Kon Ruksa Thalay. Save Andaman Network, Trang

Sato S (1996) Numerical simulation of 1993 Southwest Hokkaido earthquake tsunami around Okushiri Island. J Waterw Port Coast Ocean Eng. 122(5):209–215

Satake K (1988) Effect of bathymetry on tsunami propagation: application of ray tracing to tsunamis. PAGEOPH 126(1):27–36

Shokin YI, Chubarov LB, Novikov VA, Sudakov AN (1987) Calculations of tsunami travel times charts in the Pacific Ocean (models, algorithms, techniques, results). Sci Tsunami Hazards 5(2):85–113

Sloss PW (2005) ETOPO2 global 2-minute gridded elevation data. http://www.ngdc.noaa.gov/mgg/global/relief/ETOPO2/readme.txt. Cited 25 May 2007

Sterman JD (2000) Business dynamics: system thinking and modeling for a complex world. McGraw-Hill, Singapore

Tsuji Y, Namegaya Y, Matsumoto H, Iwasaki S, Kanbua W, Sriwichai M, Meesuk V (2006) The 2004 Indian tsunami in Thailand: surveyed runup heights and tide gauge records. Earth Planets Space 58(2):223–232

Titov V, González FI, Mofjeld HO, Newman JC (2001) Project SIFT (Short-term inundation forecasting for tsunamis). In: Proceedings of the international tsunami symposium 2001, Seattle, WA, 7–10 August 2001, pp 715–721

Thomson JM (2005) Thailand tsunami—my experience in Khao Lak—26 December 2004. http://www.sonomacountylaw.com/tsunami/timeline.htm. Cited 27 May 2007

TMD (Thai Meteorology Department) (2006) Project of installing three tsunami measurement stations under National Disaster Warning Center Project (No. 2). http://www.gprocurement.go.th/06_tor/uploads/4491/1/Tsunami.pdf

Wessel P (2005) TTT (Tsunami travel time) software, version 3.0. http://www.geoware-online.com. Cited 1 May 2007

Ventana Systems (2007) Vensim® 5 User's guide, Ventana Systems, Harvard

Yeh H, Liu P, Briggs M, Synolakis C (1994) Propagation and amplification of tsunamis at coastal boundaries. Nature 372:353–355